

Failure Analysis of the Johnson Screen in Ammonia Converter 105-D at Plant Area I B. PT Petrokimia Gresik Using the Finite Element Method

¹Syaiful, ²Eflita Yohana

^{1,2}Dept. of Mechanical Engineering, Diponegoro University, Jl. Prof. Sudarto No. 13, Tembalang, Kec. Tembalang, Semarang, Central Java 50275, Indonesia

E-mail: radityafirdaus0303@gmail.com, syaiful.undip2011@gmail.com

Abstract - PT Petrokimia Gresik is one of the largest fertilizer and chemical producers in Indonesia. In addition to fertilizer production, the industry manufactures various other chemical products, notably ammonia gas. PT Petrokimia Gresik utilizes an ammonia converter unit as a critical component in the ammonia production process. The ammonia converter serves as a reactor designed to synthesize nitrogen (N₂) and hydrogen (H₂) into ammonia (NH₃) gas, employing a catalyst as a medium to accelerate the chemical reaction. This synthesis is an exothermic process that generates significant heat; consequently, the internal material components are required to possess superior high-temperature resistance characteristics. Field observations have identified damage to the Johnson screen, which functions as a catalyst support within the converter. This failure leads to catalyst leakage and a subsequent reduction in operational efficiency. This study aims to analyze the underlying causes of the damage and evaluate the material durability of the Johnson screen through an engineering design approach and structural analysis utilizing simulation software.

Keywords: Ammonia converter, Johnson screen, stainless steel 316, structural analysis, failure theory.

I. INTRODUCTION

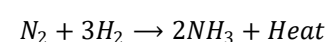
Indonesia is an agrarian nation where a significant portion of the population derives income from cultivation or farming. This indicates that the agricultural sector plays a vital role in the welfare of fundamental food requirements. The population in Indonesia continues to grow annually and this consequently increases the demand for food. In this regard, the agricultural sector also expands, leading to a higher necessity for fertilizers [1].

The fertilizer production process involves various chemical and physical stages including raw material processing, mixing, chemical reactions, purification, and packaging [2,3]. Production processes in this industry utilize

various advanced technologies and complex operating systems. However, within such complexity, the potential for operational issues such as equipment damage, system failures, or product quality problems represents a significant challenge [4].

One aspect of these processes is the production of ammonia (NH₃) gas. This gas is the primary raw material for urea, ammonium nitrate, and various other chemical compounds. The ammonia formation itself undergoes chemical processes within the ammonia converter. The ammonia converter is a crucial apparatus in ammonia production, particularly in the Ammonia Unit of Plant I B, where the equipment facilitates the process known as the Haber Bosch process.

The Haber Bosch process is the primary industrial method for ammonia (NH₃) synthesis by converting atmospheric nitrogen (N₂) and hydrogen (H₂) into ammonia using a metallic catalyst, typically iron, under elevated temperatures. This process is conducted at temperatures ranging from 400 to 500°C to ensure the reaction proceeds at an optimal rate while considering chemical equilibrium. This is necessary because the reaction is exothermic and the equilibrium is more favourable at lower temperatures. Therefore, high temperatures are employed to accelerate the ammonia gas synthesis reaction [5]. The combination of nitrogen (N₂) and hydrogen (H₂) is facilitated through the catalytic reaction of a metallic catalyst to produce ammonia gas (NH₃) with a ratio of 1 to 3 [6]. The ammonia synthesis reaction between nitrogen and hydrogen is provided below [7].



The ammonia converter reactor significantly influences the productivity and efficiency of an ammonia plant, as evidenced by the increase in NH₃ production output from the apparatus [8].

Within the ammonia converter vessel, there is a Johnson screen located in every bed. The Johnson screen functions to support the catalyst to ensure it remains in position so that gas reacts uniformly as it passes through the catalyst [9]. This process involves extreme conditions because it is exothermic and generates heat. The temperature can reach approximately 400°C [10]. Consequently, based on these extreme conditions, materials with high mechanical strength plus resistance to creep and corrosion at high temperatures are required [11].

Damage occurred in ammonia converter 105 D, involving a leak in the catalyst support section, where the primary cause was the deformation of the Johnson screen. This situation caused catalyst leakage into the lower part of the vessel bed, resulting in uneven gas distribution during the reaction process and a reduction in ammonia production efficiency. This report focuses on the analysis of wiremesh material durability against high temperatures and provides recommendations to strengthen that specific section. The durability of the material used for the wiremesh in ammonia converter 105 D must be reanalyzed to identify alternative solutions [12].

Finite Element Analysis or FEA divides a complex substance into several finite units, which are then connected by nodes. These elements are processed computationally to study their characteristics [13]. Utilizing FEA to simulate combined thermal loading on components within the reactor vessel emphasizes the importance of material selection based on yield strength, thermal conductivity and thermal expansion coefficients [14]. The Finite Element is also an effective simulation for solving numerical problems related to cracks or fracture strength [15].

The objective of this research is to find solutions to a specific problem. This problem involves the analysis process of damage to the Johnson screen at PT Petrokimia Gresik Ammonia Plant I B, which experienced leakage caused by structural deformation due to thermal loads. The analysis process begins with the three-dimensional design of the Johnson screen using the SolidWorks 2023 application according to the data.

Subsequently, the structural analysis process uses the Ansys Workbench 2020 R2 application to obtain strength indices such as equivalent elastic strain plus equivalent stress and total deformation, along with the safety factor. The study also aims to identify the critical point of highest stress on the Johnson screen and determine the reasons why the component is considered to have failed as shown in Figure 1.

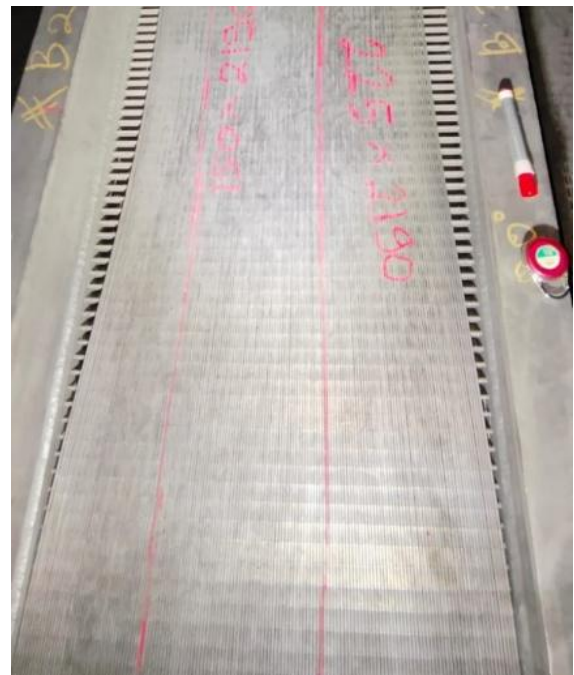


Figure 1: Johnson screen is damaged

II. RESEARCH METHODOLOGY

This section describes the methodology employed in conducting the analysis. The research process commences with problem identification to determine the primary issues to be investigated. Subsequently, a literature review is performed to establish a theoretical foundation and gather references relevant to the research topic. The next stage involves collecting the necessary data as input for the analysis. The acquired data is then utilized in the geometric design phase, where the component model or shape is drafted according to the actual component design. Following this, simulations are executed to determine the response or behaviour of the design under specified conditions. The simulation results are then evaluated during the design result analysis stage to assess performance and alignment with the research objectives. Based on this analysis, conclusions are formulated as a summary of the findings, and the study concludes with recommendations based on the conducted research.

To perform an analysis regarding the damage of the Johnson screen in ammonia converter 105 D, several steps are undertaken, including identifying existing field issues and collecting data through interviews with field supervisors. Additional data is obtained from the company PT Petrokimia Gresik, along with a literature study concerning supporting data for the Johnson screen design, plus understanding the causes of catalyst support failure and its supporting theories. Interviews were also conducted with employees of the Maintenance I section at Ammonia Plant I B in PT Petrokimia Gresik. The geometric design of the Johnson screen is developed using the SolidWorks 2023 application, while

structural analysis is performed using the Ansys Workbench 2020 R2 application, followed by an analysis of the simulation results.

The deformation and stress results obtained through ANSYS simulations utilize a mathematical approach to verify platform accuracy. It is concluded that FEA software is beneficial for designing and analyzing such components. The FEA results are also found to be consistent with mathematical model outcomes. After performing an extensive literature survey, it was determined that component dimensions are designed and analyzed using specialized analysis software. Thermal and structural loads are considered as boundary conditions for the simulation. Materials used in the actual components are treated as input parameters.

From the available literature, it is evident that comparative studies on component performance within reactor vessels using various engineering materials have not been extensively explored [16]. This study focuses on the failure analysis of stainless steel 316 material, which is utilized in structural applications under high temperature loads. The modeled Johnson screen components are subjected to high thermal loads, and their structural performance is evaluated when exposed to various temperature variations. Subsequently, the magnitude of equivalent strain plus equivalent stress and total deformation, along with the safety factor occurring in the Johnson screen, can be determined.

2.1 Problem-Solving Procedure

Following this, the magnitude of equivalent strain plus equivalent stress and total deformation, along with the safety factor occurring in the Johnson screen, can be determined. The data utilized in data processing includes the geometric model data of the Johnson screen. Geometric model data encompasses the dimensions of the Johnson screen itself. Furthermore, property data regarding the thermal load occurring on the Johnson screen during operation is incorporated [17]. The Johnson screen geometry features a vee wire wedge profile. The vee wire or wedge wire profile is selected due to its ability to form slots that narrow at the surface but widen toward the interior, which effectively prevents clogging. This profile also increases the open area for fluid flow while reducing pressure loss and distributing stress more uniformly. This design also provides superior mechanical strength when welded to the support rods, making it suitable for high-pressure and high-temperature conditions such as those found in an ammonia converter [19,20]. Geometric data for the Johnson screen are shown in Figures 2 and 3. Subsequently, the geometric specification data of the Johnson screen are presented in Table 1.

Table 1: Geometric specifications of Johnson screen

Specification	Size
length J.S	100 mm
Width J.S	37.4 mm
Width Wire	2.2 mm
Height Wire	3.5 mm
Relief angel	13°
Slot Space	1 mm

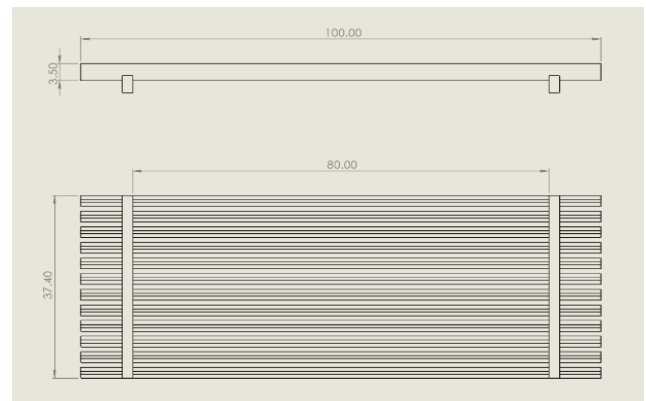


Figure 2: Johnson Screen Geometry

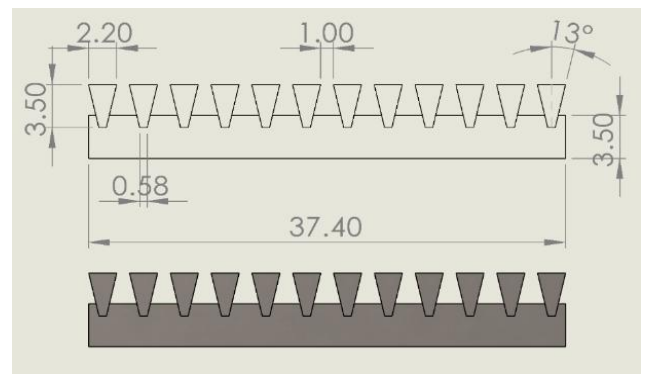


Figure 3: Vee-Wire Wedge Profile Geometry

2.2 Mathematical Model

Thermal strain (ϵ_{th}) represents the relative dimensional change of a material resulting from an increase or decrease in temperature in the absence of external forces. This phenomenon occurs because the increase in thermal energy causes atoms within the crystal lattice to vibrate more intensely and move further apart from one another, which leads to an increase in interatomic distance and subsequently causes the material to expand [20]. Thermal strain is a function of absolute temperature and the temperature-dependent coefficient of linear thermal expansion of the metal [21]. The relationship is mathematically expressed as follows:

$$\epsilon_{th} = \alpha(T) (T - T_0) \quad (1)$$

Where:

ϵ_{th} = Thermal strain

$\alpha(T)$ = Coefficient of linear thermal expansion (K^{-1})

$T - T_0$ = Temperature change (K or °C)

Stress is the primary cause of permanent deformation or thermal cracking in high-temperature metal structures such as the Johnson Screen within an ammonia converter. Thermal stress analysis is essential for predicting the elasticity limits of materials at high operating temperatures. Thermal stress (σ_{th}) arises when the strain induced by temperature changes is restricted by mechanical constraints such as joints or differences in expansion between components [22]. The mathematical relationship between strain and stress is expressed as follows:

$$\sigma = E(\epsilon_{total} - \epsilon_{th}) \quad (2)$$

If thermal expansion is perfectly restricted or under fully constrained conditions such that no deformation occurs, then the total strain is zero, and the entire strain is converted into stress:

$$\sigma_{th} = -E \epsilon_{th} = -E \alpha(T - T_0) \quad (3)$$

In the equation above, the negative sign indicates compressive stress because expansion is restricted. In the case of steady state temperature and fully constrained conditions, the maximum thermal stress is defined as follows:

$$\sigma_{th} = E(T) \alpha(T) \Delta T \quad (4)$$

Where:

σ_{th} = Thermal stress (MPa)

$E(T)$ = Modulus of Elasticity (GPa)

$\alpha(T)$ = Coefficient of linear thermal expansion (K^{-1})

$\Delta T = (T - T_0)$ = Temperature Change (K or °C)

Von Mises stress (σ_v) is a scalar quantity that represents the intensity of deformation energy within a material resulting from a combination of three principal stress components. This value is utilized to predict the initiation of plasticity in ductile materials through the yield criterion. von Mises stress does not merely consider a single force direction but also encompasses the interaction between stress components which makes it appropriate for three dimensional FEA analysis. This parameter is frequently utilized in high pressure industries such as the ammonia converter to evaluate the feasibility of a design against thermal yielding [23]. To determine whether thermal stress induces yielding the equivalent von Mises stress is applied [24]. The following is the equation:

$$\sigma_v = \sqrt{\frac{1}{2}[(\sigma_1 - \sigma_2)^2 + (\sigma_2 - \sigma_3)^2 + (\sigma_3 - \sigma_1)^2]} \quad (5)$$

Where:

σ_v = von Mises Stress (MPa)

σ_1 = First principal stress, the largest principal stress in the element (MPa)

σ_2 = Second (intermediate) principal stress (MPa)

σ_3 = Third (minimum) principal stress, which can be a compressive stress (MPa)

The Safety Factor or SF is defined as the ratio between the available material strength and the actual load experienced. The SF value indicates the extent to which a design remains secure before reaching the yield limit, where larger values signify a safer design. In FEA simulations, the SF is calculated for each element to identify critical areas with a risk of thermal failure by comparing the calculated stress with the yield strength of the material [25]. The following is the equation:

$$SF = \frac{\sigma_y}{\sigma_v} \quad (6)$$

2.3 Johnson Screen Design Simulation

Design simulation represents a vital phase in the engineering process to verify the performance and strength of a component before physical production or operation [26]. In this section, an analysis of the Johnson screen is conducted using the ANSYS 2020 software to determine the location of the peak stress on the Johnson screen and its deformation characteristics.

It is assumed that the simulation stages are performed systematically, starting from the three-dimensional modelling process, followed by material settings and the application of boundary conditions such as fixed support, as well as the meshing process and results analysis [27]. By utilizing this simulation, the author obtains results that can be further analyzed regarding the characteristics of stainless steel 316 when subjected to thermal loads, along with the identification of critical areas within the component. This simulation consists of three stages, including preprocessing, processing and postprocessing [28].

Preprocessing is the initial step in performing a numerical simulation. This stage includes several parts, such as geometry creation along with material determination, where stainless steel 316 is utilized for all Johnson screen components in accordance with company and vendor data. Furthermore, the parameters employed are defined, including an initial load of 22°C and a temperature of 400°C, while assuming fixed support is applied at the support points of the Johnson screen and the brackets to ensure the object remains stationary as in actual conditions. The final step in

preprocessing is meshing. Meshing automatically determines the optimal mesh shape for the model provided for analysis. Smart meshing has no limitations in selecting the mesh shape. The element size assigned is 0.5 mm as shown in Figure 4, and the data is presented in Table 2.

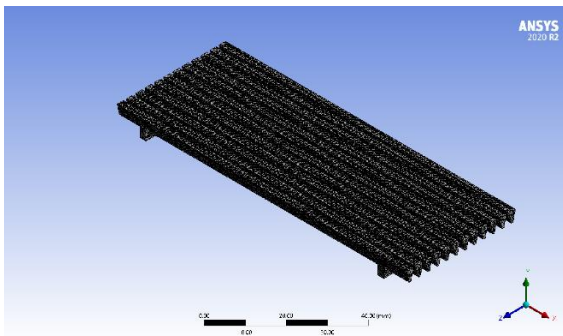


Figure 4: meshing

Table 2: Meshing Data

Element Size	0.5 mm
Element	446955
Nodes	713961

The processing stage represents the second step in this simulation, involving the execution of the simulation based on the meshed geometry within the setup section using the Ansys steady state thermal and static structural analysis software [29]. In this analysis, the initial temperature or initial load is 22°C while a thermal load of 400°C is subsequently applied to the upper surface of the Johnson screen. Gas inflow is assumed to originate from the top because the Johnson screen is located at the bottom of the bed, while the gas inlet is positioned at the top.

Conversely, the contact area between the bed and the bottom section of the Johnson screen is designated as a fixed support. This classification is based on the connection between these two components, which provides significant initial resistance to maintain the position of the Johnson screen during system operation, allowing the boundary conditions to be simplified as stationary. The placement of the boundary conditions can be observed in Figures 5 and 6.

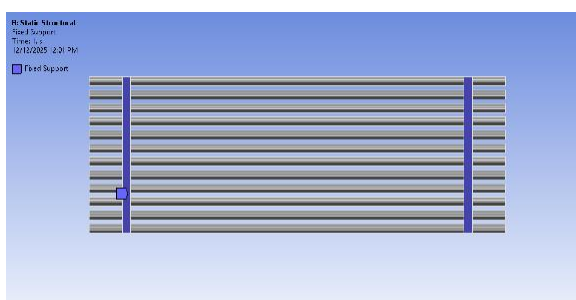


Figure 5: Boundary condition fixed support

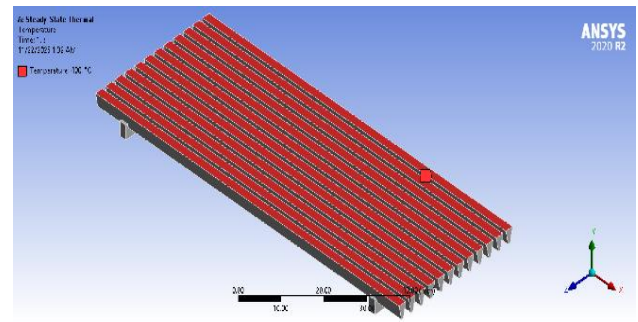


Figure 6: Boundary condition temperature

The final stage is postprocessing: Postprocessing is the phase during which simulation results are processed and analyzed to understand the structural response to the applied loads. These findings are presented as images or quantitative data to assist in decision-making. The extracted parameters include total deformation, equivalent stress and safety factor. The simulation results for the actual cover ball collector and its improvement will be presented in the results and discussion section.

III. RESULTS AND DISCUSSION

Following the completion of the simulation stages in Ansys 2020, an analysis of the results is conducted to examine the Johnson screen structure under thermal loading. The modelling approaches employed in this study consist of steady-state thermal and static structural analysis. The simulation results are illustrated in the following figures.

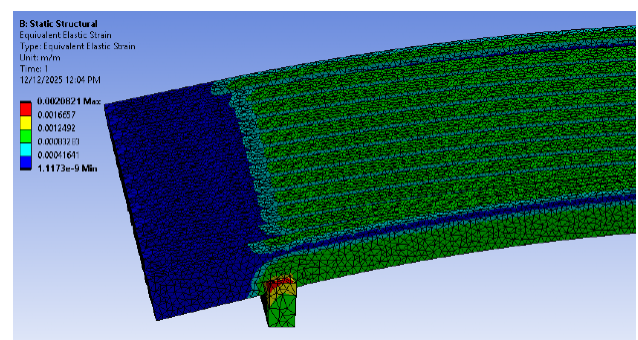


Figure 7: Equivalent elastic strain simulation result

According to the simulation findings, the maximum equivalent elastic strain on the Johnson screen structure fabricated from Stainless Steel 316 reaches approximately 0.00208. This value indicates that the deformation occurs within the elastic limits of the material. Considering the modulus of elasticity for stainless steel 316, this strain value is relatively low and suggests that the structure retains its ability to maintain its original form without permanent deformation. This confirms that the Johnson screen design is structurally sound for supporting the static loads applied during the simulation. Nevertheless, since the structure undergoes

alterations in form and dimension that impede its intended function, the component is deemed to have failed [30].

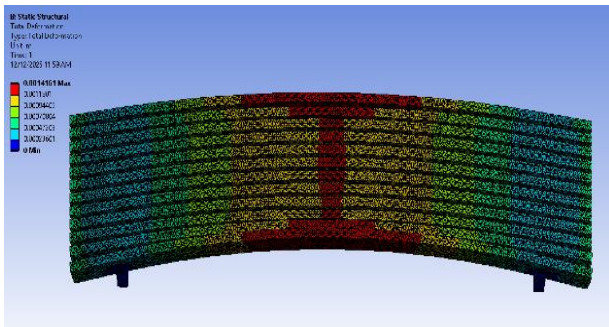


Figure 8: Total deformation simulation result

Based on the simulation results for total deformation of the Stainless Steel 316 Johnson screen structure, a maximum deformation value of 1.4161 mm was acquired in the regions represented by the red colour gradient. This indicates the most flexible area resulting from the applied loading and boundary conditions. Meanwhile, sections situated near the supports or constraints exhibit the least deformation, approaching 0 mm, which signifies the substantial influence of the boundary condition on the displacement distribution. The resulting deformation pattern aligns with the curvature of the wire geometry, indicating that the structural form significantly affects the direction and magnitude of displacement. The magnitude of this deformation is relatively small compared to the total dimensions of the component, suggesting that the structure remains sufficiently rigid and stable under the applied static loads. Nevertheless, in actual applications involving high temperatures and cyclic loading, this deformation could potentially increase. Consequently, further evaluation of thermal deformation and the possibility of material fatigue is required [31].

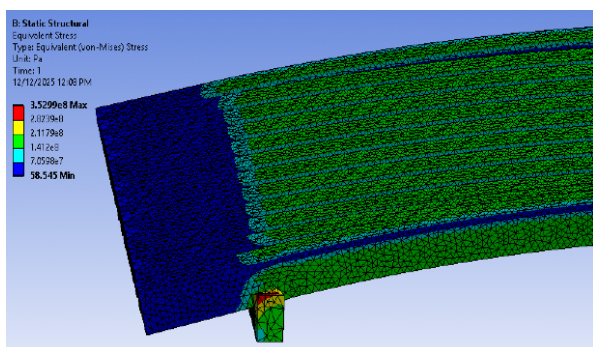


Figure 9: Equivalent stress simulation result

The simulation demonstrates that the maximum von Mises stress on the Johnson screen structure composed of Stainless Steel 316 reaches approximately 352.99 MPa. This value lies within the range of or slightly exceeds the yield strength of SS 316, depending on the material condition. The

stress distribution pattern reveals stress concentrations at the curvature areas and welded joints, which indicates that geometry and boundary conditions significantly influence the structural response. This suggests that while a major portion of the structure may undergo local plasticity, the overall design can maintain its integrity if adequate safety factors and thickness margins are provided. Nevertheless, these conditions underscore the necessity for further evaluation, particularly regarding cyclic loading plus corrosion and thermal loads to anticipate risks of premature failure such as fatigue or permanent deformation [32].

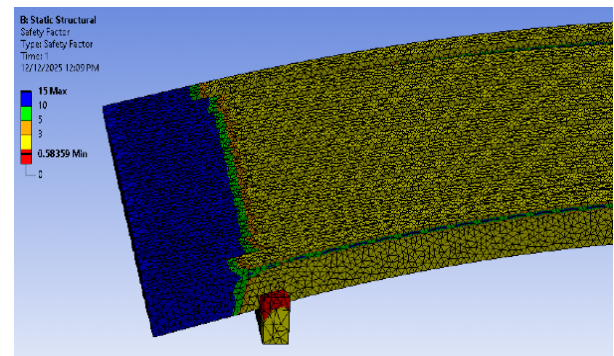


Figure 10: Safety factor simulation result

The safety factor simulation results for the Johnson screen structure composed of Stainless Steel 316 show a minimum safety factor value of approximately 0.58. This indicates that several parts of the structure are very close to or even below the ideal safety limit, which signifies a potential risk of local failure if additional loads plus dynamic conditions or thermal cycles occur [33]. This low safety factor distribution is caused by stress concentrations occurring at the Johnson screen joints, which demonstrates that geometric design and boundary conditions significantly influence structural safety. Therefore, while other sections of the component may still be within the safe zone, the minimum safety factor value signals the necessity for design revisions, such as increasing thickness, load redistribution and geometry optimization, to ensure structural integrity under actual operating conditions.

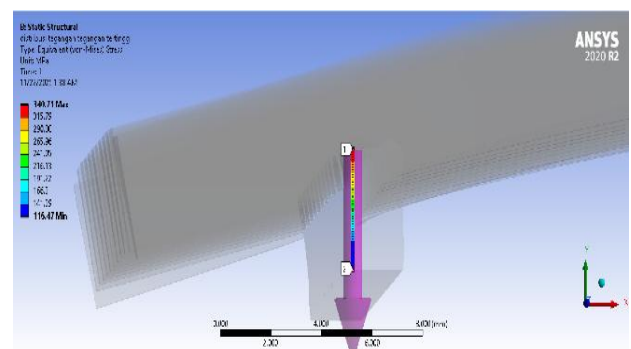


Figure 11: Distribution of parts experiencing the highest stress

At the focal joint location, a maximum von Mises stress of approximately 340.7 MPa is observed, which indicates a significant stress concentration that potentially approaches or exceeds the local yield limit of the Stainless Steel 316 material. This condition signifies a risk of local plastic deformation or damage initiation, particularly if load cycles or corrosion occur. Consequently, design improvements in that specific area, such as the addition of a fillet radius plus local thickening or load redistribution, are recommended along with further analysis to assess long term durability [34].

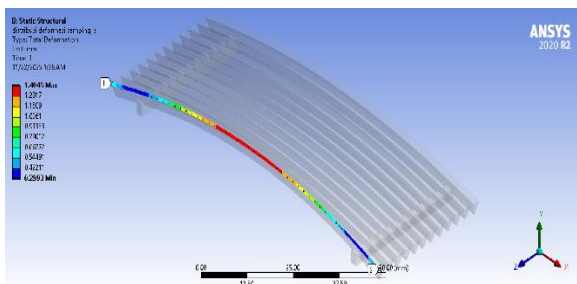


Figure 12: Distribution of deformation in the curved section

The distribution of lateral deformation on the Johnson screen indicates a maximum displacement of approximately 1.4045 mm, particularly in the wire curvature area. This signifies that the wire undergoes substantial deflection in the lateral direction. This lateral deformation can cause the wire gaps to expand, which allows catalyst particles to fall or leak into the lower part of the system. Therefore, this deflection, which is generated by the wire geometry and the constraint conditions, serves as a primary potential cause of catalyst leakage in actual applications. To prevent this occurrence, design improvements such as the addition of lateral supports, plus the reduction of wire spacing or an increase in the stiffness of the wire structure are required [35].

Subsequently, the analysis is performed across five temperature variations to examine the comparison of stainless steel 316 material properties under different thermal conditions. The corresponding graphs are illustrated in Figure 13 and Figure 14.

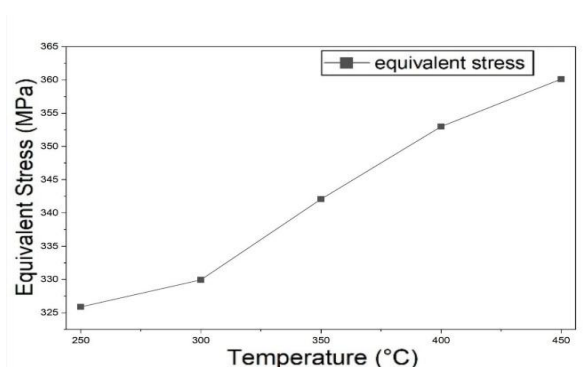


Figure 13: Comparison chart of temperature and equivalent stress

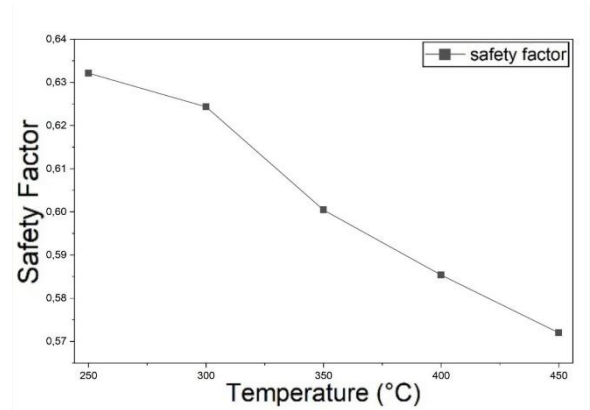


Figure 14: Comparison graph of temperature and safety factor

The analysis results indicate that the temperature increase is directly proportional to the rise in equivalent stress values within the component structure. At a temperature of 250 °C, the equivalent stress was recorded at 325.88 MPa. When the temperature increases to 300 °C, the stress rises to 329.94 MPa. This upward trend continues at 350 °C with a value of 343.08 MPa, then increases to 352.99 MPa at 400 °C and reaches the peak value of 360.13 MPa at a temperature of 450 °C.

Overall, a temperature increase of 200 °C (from 250 °C to 450 °C) causes an equivalent stress increment of 34.25 MPa or approximately 10.5 percent. This demonstrates that the thermal load contributes significantly to the stress occurring within the structure, which can elevate the risk of plastic deformation or material failure if it approaches or exceeds the yield limit of the material utilized.

The analysis results demonstrate that the temperature increase causes a consistent decrease in the safety factor value of the structure. At a temperature of 250 °C, the safety factor is 0.63214, then decreases to 0.62435 at 300 °C. A more significant reduction occurs at 350 °C with a value of 0.60044, followed by 0.58359 at 400 °C, and reaches the minimum value of 0.57202 at 450 °C.

In general, the temperature increase leads to a safety factor reduction of 0.06012 or approximately 9.5 percent. The maximum safety factor values remain below 1 across all temperature variations, which signifies that critical areas of the structure are in an unsafe condition and possess the potential for plastic deformation or failure if subjected to continuous thermal loading. This indicates that the temperature load is a critical factor that significantly diminishes the structural capacity to withstand operating loads.

IV. CONCLUSION

Based on the analysis and testing conducted, several conclusions are formulated as follows:

1. Actual damage and simulation results exhibit a consistent deformation pattern. Field findings reveal deformation in the form of shrinkage in the Johnson Screen wire, which caused catalyst leakage into the lower vessel bed. This failure pattern aligns with numerical simulation results where the maximum total deformation reaches 1.4161 mm with thermal stress distribution localized on the outer screen surface. This indicates that the Johnson Screen is indeed subjected to excessive loads at specific points, which trigger permanent deformation.
2. The performance of Stainless Steel 316 material is restricted at high operating temperatures. Based on simulation results, a maximum equivalent stress of 352.99 MPa was measured at critical areas. This value relatively approaches or even exceeds the yield strength of Stainless Steel 316, which is approximately 290 MPa at room temperature and decreases at 400 °C. A study by Nurisman, Effendi, and Septiani (2025) emphasizes that catalyst support materials in ammonia reactors must possess high creep and corrosion resistance to prevent premature failure. Consequently, it is concluded that the selection of SS 316 is less than optimal for long-term operating conditions at approximately 400 °C.
3. The safety factor values demonstrate the presence of unsafe regions. From the simulation results, the minimum safety factor reaches 0.58359, which is less than the safe limit of 1.0. This implies that certain sections of the Johnson Screen are theoretically beyond the elastic capacity of the material and are vulnerable to plastic failure. This is consistent with the Risk Based Inspection or RBI method utilized by Soelaiman, Taufik, and Soma (2004) where the ammonia converter is categorized as high-risk equipment due to temperature factors and the significant impact of failure on the production process.
4. Although the average safety factor remains above the safe range and only a small area possesses a safety factor below the safe threshold, the component is still considered failed. According to the theory from Collins in the book *Mechanical Design of Machine Elements and Machines*, published in 1981, a component is defined as failed if it undergoes changes in size, shape or material properties that render it unable to perform its intended function. In this case, the function of the Johnson Screen as a catalyst support failed because of structural deformation, which allowed catalyst particles to leak into the area below the bed or thermal barrier.

Available:

https://eprints2.undip.ac.id/id/eprint/12946/1/S_AzizahRahman.pdf

- [2] V. Pattabathula and J. Richardson, "Introduction to ammonia production," *Chem. Eng. Prog.*, vol. 112, no. 9, pp. 69–75, 2016.
- [3] A.I. Amhamed *et al.*, "Ammonia Production Plants—A Review," *Fuels*, vol. 3, no. 3, pp. 408–435, 2022, doi: 10.3390/fuels3030026.
- [4] P. Examiner and M. C. Knode, "United States Patent (19)," no. 19, 2000.
- [5] J. Humphreys, R. Lan, and S. Tao, "Development and Recent Progress on Ammonia Synthesis Catalysts for Haber–Bosch Process," *Adv. Energy Sustain. Res.*, vol. 2, no. 1, pp. 1–23, 2021, doi: 10.1002/aesr.202000043.
- [6] R. M. Yusuf Agustria, Al Azhar, and Rizka Wulandari Putri, "Evaluasi efisiensi ammonia converter unit ammonia pada industri pupuk urea," *J. Tek. Kim.*, vol. 25, no. 3, pp. 70–74, 2019, doi: 10.36706/jtk.v25i3.130.
- [7] M. Ojha and A. K. Dhiman, "Problem , Failure and Safety Analysis of Ammonia Plant : a Review," vol. 2, no. October, pp. 631–646, 2010.
- [8] D. Bahrin, I. N. Sakinah, and F. U. Kendari Putri, "Analisa Performance Ammonia Converter Pabrik Pupuk Sebelum dan Sesudah Turn Around (TA)," *J. Tek. Kim*, vol. 25, no. 1, pp. 13–17, 2019, doi: 10.36706/jtk.v25i1.15.
- [9] "johnson screens technical information Architecture and Construction johnson screens technical information Architecture and Construction".
- [10] E. Nurisman, Y. Effendi, and N. Septiani, "Analysis of factors influencing the performance of the ammonia converter at plant IIB of PT Pupuk Sriwidjaja," *Sainteks J. Sain dan Tek.*, vol. 7, no. 01, pp. 88–98, 2025, doi: 10.37577/sainteks.v7i01.701.
- [11] P. Baboo, "A CASE STUDY FOR FAILURE IN AMMONIA SYNTHESIS CONVERTER & TROUBLE FOR FAILURE IN AMMONIA SYNTHESIS," no. December, 2015.
- [12] "Jurnal Teknik Mesin Volume XIX - No . 2 - Oktober 2004," vol. XIX, no. 2, 2004.
- [13] "What is Finite Element Analysis (FEA)? | Ansys." [Online]. Available: <https://www.ansys.com/simulation-topics/what-is-finite-element-analysis>
- [14] D. Shrivastava and P. A. Dubey, "FEM Enabled Structural and Steady State Analysis," no. September, 2025.
- [15] S. N. Butt and G. Meschke, "Peridynamic analysis of dynamic fracture : influence of peridynamic horizon, dimensionality and specimen size," *Comput. Mech.*,

REFERENCES

- [1] A. Rahman, "Desain Proyek Pabrik Asam Nitrat Dengan Proses Ostwald High-Single Pressure Kapasitas 88.000 Ton/Tahun," 2022, [Online].

- vol. 67, no. 6, pp. 1719–1745, 2021, doi: 10.1007/s00466-021-02017-1.
- [16] S. S. Salins, M. Mohan, and C. Stephen, “Annales de Chimie - Science des Matériaux Finite Element Investigation on the Performance of Pressure Vessel Subjected to Structural Load,” vol. 45, no. 3, pp. 201–205, 2021.
- [17] V. Mykhailiuk, M. Liakh, R. Deineha, O. Matviienkiv, J. Pawlik, and D. Dzienniak, “OPTIMIZATION OF THE SUPPORT,” no. 202, 2024.
- [18] M. Zielina, A. Pawłowska-salach, and K. Kaczmariski, “applied sciences Hydraulic Analysis of a Passive Wedge Wire Water Intake Screen for Ichthyofauna Protection,” 2023.
- [19] “INTERNALS FOR DOWN FLOW REACTORS”.
- [20] S. Raju, “Thermal expansion studies on Inconel-600 by high temperature X-ray diffraction q,” vol. 325, pp. 18–25, 2004, doi: 10.1016/j.jnucmat.2003.10.007.
- [21] Y. Zhu and G. Chen, “Quantifying thermal strain of steel plate subjected to constant temperature by distributed fiber optic sensors,” no. July, pp. 1–13, 2022.
- [22] H. Laribou and A. Elbasset, “Numerical Study of the Thermo-mechanical Behavior of 304L Stainless Steel Pipeline Junctions,” vol. 9, no. 3, pp. 155–168, 2021, doi: 10.12691/ijp-9-3-3.
- [23] R. C. Juvinall and K. M. Marshek, *No Title*.
- [24] A. Hussein, L. Hao, C. Yan, and R. Everson, “Finite element simulation of the temperature and stress fields in single layers built without-support in selective laser melting,” *Mater. Des.*, vol. 52, pp. 638–647, 2013, doi: 10.1016/j.matdes.2013.05.070.
- [25] A. Fathurrahman, S. H. Suryo, D. T. Mesin, F. Teknik, and U. Diponegoro, “ANALISIS SIFAT MEKANIK DAN OPTIMALISASI STRUKTUR BOOM EXCAVATOR V EC650BE MENGGUNAKAN METODE ELEMEN HINGGA,” vol. 10, no. 3, pp. 405–414, 2022.
- [26] A. Papanikolaou, E. Boulougouris, S. Erikstad, S. Harries, and A. A. Kana, “Ship Design in the Era of Digital Transition - A State-of-the-Art Report,” pp. 0–2, 2024.
- [27] R. Paul and V. L. Chowdary, “AND ENGINEERING TRENDS DESIGN AND STATIC ANALYSIS OF DIFFERENT PRESSURE VESSELS AND MATERIALS USING FEM METHOD,” vol. 5, no. 7, pp. 93–99, 2020.
- [28] Y. Zhao, “The Pre and Post-Processing in Finite Element Analysis on the Technology and Programming of Plane Reinforced Concrete Based on AutoCAD Platform,” no. Meici, pp. 882–888, 2015.
- [29] M. Ernesto, G. Rivera, L. David, and C. Garcia, “Thermal – Structural Linear Static Analysis of Functionally Graded Beams Using Reddy Beam Theory,” 2023.
- [30] J. A. Collins, H. R. Busby, and G. H. Staab, *Mechanical Design of Machine Elements and Machines: A Failure Prevention Perspective*. Wiley, 2009. [Online]. Available: <https://books.google.co.id/books?id=909-5C4eyUkC>
- [31] A.H. Manufacturing, X. Wu, W. Zhu, and Y. He, “Deformation Prediction and Experimental Study of 316L Stainless Steel Thin-Walled Parts Processed by,” 2021.
- [32] B. Barkia *et al.*, “Journal of Materials Science & Technology On the origin of the high tensile strength and ductility of additively manufactured 316L stainless steel: Multiscale investigation,” vol. 41, pp. 209–218, 2020, doi: 10.1016/j.jmst.2019.09.017.
- [33] K. Tanriver, A. Etyemez, and M. Ay, “Integrated use of finite element analysis and gaussian process regression in the structural analysis of AISI 316 stainless steel chimney systems,” 2025.
- [34] I. Ríos *et al.*, “Compressive Behavior of 316L Stainless Steel Lattice Structures for Additive Manufacturing: Experimental Characterization and Numerical Modeling,” pp. 1–18, 2025.
- [35] M. Iwaniszyn, K. Sinder, A. Gancarczyk, and B. Leszczy, “Characterization of Fluid Flow and Heat Transfer of Expanded Metal Meshes for Catalytic Processes,” 2022.

Citation of this Article:

Syaiful, & Eflita Yohana. (2026). Failure Analysis of the Johnson Screen in Ammonia Converter 105-D at Plant Area I B. PT Petrokimia Gresik Using the Finite Element Method. *International Research Journal of Innovations in Engineering and Technology - IRJIET*, 10(5), 140-148. Article DOI <https://doi.org/10.47001/IRJIET/2026.105019>
